

LETTER

## Quasi-ice-like $C_p$ behavior of molecular $H_2O$ in hemimorphite $Zn_4Si_2O_7(OH)_2 \cdot H_2O$ : $C_p$ and entropy of confined $H_2O$ in microporous silicates

CHARLES A. GEIGER<sup>1,\*</sup> AND EDGAR DACHS<sup>2</sup>

<sup>1</sup>Institut für Geowissenschaften, Abteilung Mineralogie, Christian-Albrechts-Universität zu Kiel, D-24098 Kiel, Germany

<sup>2</sup>Fachbereich Materialforschung und Physik, Abteilung Mineralogie, Universität Salzburg, Hellbrunnerstrasse 34, A-5020 Salzburg, Austria

### ABSTRACT

Hemimorphite,  $Zn_4Si_2O_7(OH)_2 \cdot H_2O$ , and its dehydrated analog  $Zn_4Si_2O_7(OH)_2$  were studied by low-temperature relaxation microcalorimetry and their heat capacity determined to analyze the behavior of the confined  $H_2O$  between 5 and 300 K. An analysis of the data, which are corrected for the presence of a phase transition, shows that the  $C_p$  of  $H_2O$  in hemimorphite behaves more similar to the  $C_p$  of ice than to liquid water or steam. The  $H_2O$  molecule, with its four planar hydrogen bonds in hemimorphite, as well as its tetrahedral coordination in ice, is more rigidly hydrogen bonded in both than in liquid water. This is reflected in their respective  $C_p$  behavior. The heat capacity and entropy for the dehydration reaction at 298 K are  $\Delta C_p^{\text{rxn}} = -2.1 \pm 3.6 \text{ J/(mol}\cdot\text{K)}$  and  $\Delta S^{\text{rxn}} = 134.7 \pm 4.0 \text{ J/(mol}\cdot\text{K)}$ .  $C_p$  behavior at  $0 < T < 300 \text{ K}$  and entropy values at 298 K for confined  $H_2O$  in hemimorphite and hydrous Mg cordierite are compared to those in several zeolites. The entropy for confined  $H_2O$  in hemimorphite, analcime, and mordenite is around 54 J/(mol·K) at 298 K. The strength of the interactions (e.g., H bonding) between an  $H_2O$  molecule and its surroundings increases approximately from steam > cordierite > analcime > hemimorphite ≥ mordenite > heulandite ≈ natrolite ≈ scolecite > liquid  $H_2O$  > ice and, in the case of microporous silicates, is inversely proportional to the  $S$  of the confined  $H_2O$ .

**Keywords:** Hemimorphite, heat capacity, entropy, microporous minerals, confined  $H_2O$

### INTRODUCTION

The  $H_2O$  molecule and hydrogen bonding play a key role in many geologic processes. Certain micro/nanoporous silicates offer the possibility for one to investigate the nature of confined  $H_2O$  and hydrogen bonding at a relatively simple, yet fundamental level. One such silicate, hemimorphite,  $Zn_4Si_2O_7(OH)_2 \cdot H_2O$ , has been studied in terms of its crystal structure several times at different temperatures using both single-crystal X-ray and neutron diffraction (see Taylor 1962; Hill et al. 1977; Cooper et al. 1981; Libowitzky et al. 1998). Its structure has a single, confined  $H_2O$  molecule that is held in place only through hydrogen bonding. Complementary single-crystal IR absorption and Raman spectroscopic studies have provided vibrational properties of the  $H_2O$  molecule and information on the strength of the hydrogen bonding to the framework (Libowitzky and Rossman 1997; Kolesov 2006). Hemimorphite shares certain similarities with zeolites, because they also have  $H_2O$  molecules located in channel ways that are hydrogen bonded with their crystal frameworks and/or with each other, but differ in that their  $H_2O$  molecules are also bonded to extra-framework cations. In addition, the  $H_2O$  in hemimorphite can be removed without disruption of the framework structure, but it is not reversibly reabsorbed as in the zeolites.

To study confined  $H_2O$  and hydrogen bonding in hemimorphite, thermodynamic behavior, especially heat capacity at  $0 < T < 300 \text{ K}$ , is of special interest. Because hydrogen bonding associated with confined  $H_2O$  is a relatively weak force in most silicates, it will express itself in  $C_p$  at low temperatures. Calorimetric work has been undertaken for several natural zeolites

(e.g., Johnson et al. 1982, 1983, 1985, 1992; Paukov et al. 2002) and these studies show that the  $C_p$  contribution and the entropy,  $S$ , at 298 K of  $H_2O$  in zeolites are variable. In spite of this reported variability, thermodynamic studies (e.g., Helgeson et al. 1978; Robinson and Haas 1983; Van Hinsberg et al. 2005) have proposed “standard values” of  $S$  for confined  $H_2O$  in a variety of microporous silicates for use in calculations and databases.

Few heat capacity studies at low temperatures have been reported for non-zeolitic hydrous microporous silicates (see Paukov et al. 2007 for work on cordierite). More calorimetric work needs to be undertaken on a greater variety of phases to fully understand the thermodynamic properties of their confined  $H_2O$ . The new data reported here on hemimorphite, together with previously published calorimetric results on related phases, permit an analysis of  $C_p$  and  $S$  behavior of confined  $H_2O$  and their relationship to hydrogen bonding in microporous silicates.

### EXPERIMENTAL METHODS

#### Sample, characterization, and calorimetry

The hemimorphite investigated is from the Ojuela Mine, Mapimi, Durango, Mexico (University of Kiel mineral collection). Two euhedral, colorless and transparent, crystals 5–10 mm in size were separated from their underlying matrix. Electron microprobe analysis showed only the presence of Zn and Si. The crystals were ground in an agate mortar to obtain roughly 400 mg of sample. X-ray powder diffraction measurements using a Siemens D-5000 diffractometer with  $0.1^\circ$  step scans every 10 s between 10 and  $60^\circ 2\theta$  showed only reflections that could be indexed to hemimorphite. A 100 mg fraction was used for heating experiments to expel the confined  $H_2O$ . It was placed in an open Au capsule, heated in air at  $50 \text{ K/h}$  to 748 K, and held for 6 h using a tube furnace with a temperature control of  $\pm 1 \text{ K}$ , which was also checked by an external Cr-CrNi thermocouple. Following heating, the sample was removed from the furnace, cooled, and characterized by X-ray powder diffraction. The X-ray powder diffraction pattern of the dehydrated hemimorphite also matches well that calculated from the single-crystal data of

\* E-mail: chg@min.uni-kiel.de

Libowitzky et al. (1997). X-ray patterns for the natural and heat-treated samples are shown in Figure 1<sup>1</sup>.

Low-temperature heat capacities were measured with a commercial relaxation calorimeter, i.e., the Physical Properties Measurement System (PPMS) made by Quantum Design. Measurements were made between 5 and 300 K on 20.2 mg of hemimorphite and 22.5 mg of dehydrated hemimorphite held in a covered Al-container.  $C_p$  data were collected at 60 temperatures on cooling with a logarithmic or linear spacing, with  $C_p$  determined three times at each temperature. Details behind the PPMS method, as well as description of the data acquisition and evaluation procedures and error analysis, are given in Dachs and Bertoldi (2005), Dachs and Geiger (2006), and Benisek and Dachs (2008).

## RESULTS

Raw  $C_p$  data for both natural and heat-treated hemimorphite are given in Tables 1a and 1b<sup>1</sup>, and they each show evidence for a phase transition around 102 and 86 K, respectively. The phase transition in hemimorphite has been studied and will be discussed briefly below, whereas the phase transition in dehydrated hemimorphite is new. For this study, we excluded the  $C_p$  data between 54–120 K that encompasses these phase transitions to focus our analysis on the difference in  $C_p$  between the two samples that describes the behavior of the confined H<sub>2</sub>O. Thus, the raw  $C_p$  data for the natural and the heated-treated sample below and above 54–120 K were fitted to the equation (Boerio-Goates et al. 2002):

$$C_p = 3R[n \cdot D(\theta_D) + m \cdot E(\theta_E) + n_s \cdot S(\theta_S)], \quad (1)$$

where  $D(\theta_D)$ ,  $E(\theta_E)$ , and  $S(\theta_S)$  are Debye, Einstein, and Schottky functions, respectively, and  $n$ ,  $m$ ,  $n_s$ ,  $\theta_D$ ,  $\theta_E$ , and  $\theta_S$  are adjustable parameters. The resulting fitted  $C_p$  values are given in Table 2<sup>1</sup>. Using Equation 1, the experimental heat capacities above and below the transitions could be reproduced within  $0.35 \pm 0.28\%$  at  $10 < T < 54$  K and within  $0.25 \pm 0.2\%$  at temperatures above 120 K. The values between 54 and 120 K were interpolated. The third-law entropies for hemimorphite and dehydrated hemimorphite were obtained by appropriate integration of Equation 1.

## DISCUSSION

### Hemimorphite structure, confined H<sub>2</sub>O, and quasi-ice-like $C_p$ behavior

The crystal structure of hemimorphite is a framework of corner-sharing Si<sub>2</sub>O<sub>7</sub> dimers and ZnO<sub>3</sub>OH tetrahedra. The room-temperature orthorhombic *Imm*2 structure is shown in Figure 2a. Cavities are connected via six-membered rings of tetrahedra to form infinite channel ways running parallel to the *c*-axis. A single H<sub>2</sub>O molecule within each cavity has four coplanar

hydrogen bonds, located in the (010) plane, to the surrounding crystal framework. The H-bonding arrangement is unusual for a silicate because the H<sub>2</sub>O molecule acts as both a hydrogen-bond acceptor and donor. The structure of hemimorphite and the effect of elevated temperatures and dehydration were studied by Taylor (1962) and Cooper et al. (1981). The low-temperature structure was investigated by Libowitzky et al. (1998). At  $T > 300$  K, the framework undergoes only minor adjustments with loss of the H<sub>2</sub>O molecule and even retains the same symmetry when all the H<sub>2</sub>O molecules are removed to become Zn<sub>4</sub>Si<sub>2</sub>O<sub>7</sub>(OH)<sub>2</sub> (Cooper et al. 1981). Dehydroxylation of Zn<sub>4</sub>Si<sub>2</sub>O<sub>7</sub>(OH)<sub>2</sub> to  $\beta$ -Zn<sub>2</sub>SiO<sub>4</sub> begins around 933 K (Taylor 1962).

At  $T < 300$  K, the hemimorphite structure undergoes a phase transition at about 102 K, changing to the symmetry *Abm*2. The low-temperature structure has an ordered arrangement of non-equivalent hydroxyl groups and rotated water molecules, which doubles the *b*-axis (Libowitzky et al. 1998). In contrast, the low-temperature structure of dehydrated hemimorphite retains the *Imm*2 structure (Libowitzky et al. 1997). In that study, the crystal structure was refined at 110 and 293 K, single-crystal polarized FTIR spectra measured between 82 and 373 K, and optical birefringence measured between 83 and 373 K, but no phase transitions were observed. Our calorimetry work on dehydrated hemimorphite does indicate a phase transition at about 86 K, but this will be discussed elsewhere. For this study, the heat capacity contribution due to these phase transitions has been effectively removed by interpolating a smooth temperature dependence of  $C_p$  through that temperature region.

The  $C_p$  and the third-law entropy,  $S^\circ$ , at 298 K for hemimorphite and the dehydrated phase are given in Table 3. Raw  $C_p$  data and the fitted values using Equation 1 are shown in Figure 3. To obtain  $C_p$  for the confined H<sub>2</sub>O in hemimorphite, we subtracted the fitted  $C_p$  values of the heat-treated sample from the fitted  $C_p$  values of untreated hemimorphite (Fig. 3). Also plotted are the  $C_p$  values for ice and super-cooled liquid water and steam. Of the three different H<sub>2</sub>O phases, the  $C_p$  behavior of H<sub>2</sub>O in hemimorphite is most similar to that of ice at  $0 < T < 270$  K. The

<sup>1</sup> Deposit item AM-09-021, Figure 1, Tables 1a, 1b, and 2. Deposit items are available two ways: For a paper copy contact the Business Office of the Mineralogical Society of America (see inside front cover of recent issue) for price information. For an electronic copy visit the MSA web site at <http://www.minsocam.org>, go to the American Mineralogist Contents, find the table of contents for the specific volume/issue wanted, and then click on the deposit link there.

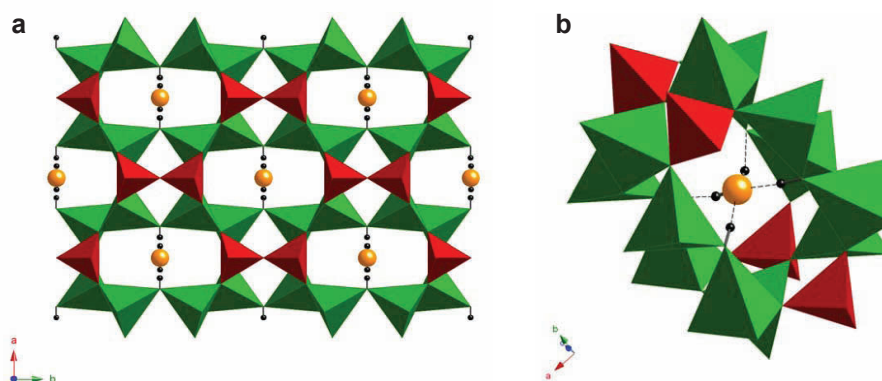


**FIGURE 2.** (a) Hemimorphite structure at 300 K. The green tetrahedra represent the ZnO<sub>3</sub>(OH) groups and the red, SiO<sub>4</sub> groups. The orange spheres are the O atoms of the H<sub>2</sub>O molecules and the small black spheres are H atoms. (b) Cavity around the H<sub>2</sub>O molecule showing the hydrogen bonds as dashed lines.

**TABLE 3.** Heat capacity and standard third-law entropy,  $S^\circ$ , at 298.15 K of hemimorphite and dehydrated hemimorphite

Sample	$C_p$ [J/(mol·K)]	$S^\circ$ [J/(mol·K)]
hemimorphite	$324 \pm 2$	$368 \pm 3$
dehydrated hemimorphite	$288 \pm 2$	$314 \pm 2$

H<sub>2</sub>O molecule in hemimorphite as well as in ice, but not as in liquid H<sub>2</sub>O, is characterized by a relatively strong arrangement of hydrogen bonds. The confined H<sub>2</sub>O in hemimorphite behaves like “quasi-two-dimensional ice,” in contrast to the tetrahedrally coordinated H<sub>2</sub>O molecules in hexagonal ice.

The heat capacity and entropy for the dehydration reaction,  $\Delta C_p^{\text{rxn}}$  and  $\Delta S^{\text{rxn}}$ , at 298 K:



were calculated using the values in Table 3, along with thermodynamic properties for ideal gaseous H<sub>2</sub>O. We obtain  $\Delta C_p^{\text{rxn}} = -2.1 \pm 3.6 \text{ J/(mol·K)}$  and  $\Delta S^{\text{rxn}} = 134.7 \pm 4.0 \text{ J/(mol·K)}$ . The entropies of ice sublimation and water vaporization at 298 K are  $\Delta S^{\text{sub.}} = 146.95 \text{ J/(mol·K)}$  and  $\Delta S^{\text{vap.}} = 118.89 \text{ J/(mol·K)}$ , respectively (Table 4). The entropy of dehydration of hemimorphite lies between the entropy of water vaporization and ice sublimation.

#### The system H<sub>2</sub>O and confined H<sub>2</sub>O in selected micro/nanoporous silicates: Thermodynamic, hydrogen-bonding, and vibrational behavior

To analyze the thermodynamic, bonding, and vibrational behavior of confined molecular H<sub>2</sub>O in silicates, the pure H<sub>2</sub>O system can be used as a reference state. Eisenberg and Kauzmann (1969) discuss the structures, vibrational states and thermodynamic properties of gaseous, liquid, and solid H<sub>2</sub>O. An important difference between liquid and solid H<sub>2</sub>O and gaseous H<sub>2</sub>O (steam) is the presence of hydrogen bonding (Jeffrey 1997) in the first two phases.

Comprehensive understanding of the thermodynamic behavior of confined H<sub>2</sub>O in micro/nanoporous minerals is lacking, whereas data exist for specific zeolites (e.g., Johnson et al. 1982, 1983, 1985, 1992; Paukov et al. 2002). Several attempts have been made to estimate or calculate  $S$  values for H<sub>2</sub>O in microporous silicates. In some treatments, “standard transferable”  $S$  values have been proposed. Helgeson et al. (1978) estimated, based on older calorimetric data for analcime and dehydrated analcime, an entropy value of “zeolitic” H<sub>2</sub>O for silicates to be 59 J/(mol·K) at 298 K. Robinson and Haas (1983) proposed a value of 54.0 J/(mol·K) for a “fictive hydrate component” (i.e., H<sub>2</sub>O) in their empirical

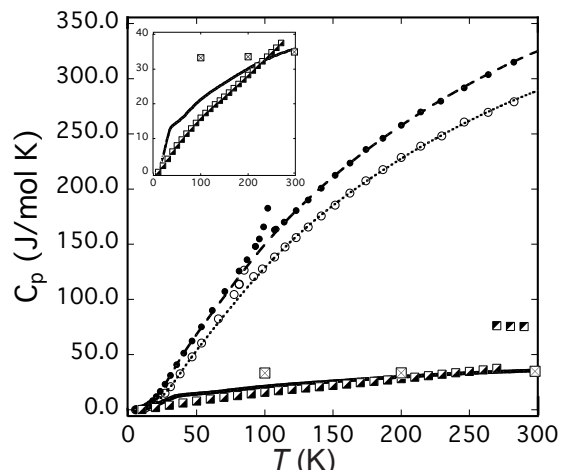


**FIGURE 3.** Heat capacity of natural and heat-treated hemimorphite (using selected raw data from Table 1), filled and open circles, respectively. The symbols are larger than the experimental uncertainty.  $C_p$  values for both phases from Equation 1 are shown as long and short dashed lines, and the lower solid line is the difference between them (i.e.,  $C_p$  of H<sub>2</sub>O in hemimorphite). The squares with the filled lower half are ice (Giauque and Stout 1936), the squares with the filled upper half are super-cooled liquid water (Angell et al. 1982) and the squares with crosses are super-cooled steam (from Paukov et al. 2007). The inset shows  $C_p$  of confined H<sub>2</sub>O in hemimorphite (line) compared to ice and steam.

procedure for calculating the entropy of various minerals. More recently, Van Hinsberg et al. (2005) obtained a lower value of  $S = 44.1 \text{ J/(mol·K)}$  for “free interstitial” H<sub>2</sub>O at 298 K in their thermodynamic analysis of silicate phases. For various H<sub>2</sub>O-containing inorganic salts, experimental entropy values of their confined H<sub>2</sub>O are roughly around 42 J/(mol·K) (see Dunitz 1994).

Table 4 lists  $C_p$  and  $S$  values at 298 K for the three most common H<sub>2</sub>O phases and for confined H<sub>2</sub>O in various micro/nanoporous silicates. For the latter,  $C_p$  varies considerably, as does  $S$  with values between 32 and 80 J/(mol·K). There is no “standard value” for either function. For confined H<sub>2</sub>O in silicates, hemimorphite, analcime, and mordenite have similar entropy values around 54 J/(mol·K), which lies between that of ice and liquid H<sub>2</sub>O. The entropy for H<sub>2</sub>O in heulandite and paranatrolite are less, namely 50.1 and 45.8 J/(mol·K), respectively. Each H<sub>2</sub>O molecule in the two small-pore zeolites natrolite and scolecite has an entropy of approximately 32 J/(mol·K), which is the lowest entropy value reported for confined molecular H<sub>2</sub>O in silicates. Hydrous Mg-cordierite is at the other extreme; its  $S$  value of 80.5 J/(mol·K) for H<sub>2</sub>O is greater even than that of liquid H<sub>2</sub>O.

We now consider  $C_p$  behavior at  $0 < T < 300 \text{ K}$ . In the case of cordierite, its  $C_p$  for H<sub>2</sub>O at  $100 < T < 300 \text{ K}$  is most similar to that of steam (see Fig. 8 in Paukov et al. 2007). As described above, H<sub>2</sub>O in hemimorphite is more ice-like. For analcime and mordenite  $C_p$  is most similar to that of ice below 50 K, but above 50 K their  $C_p$  values for H<sub>2</sub>O show larger and increased

**TABLE 4.** Heat capacity, entropy, and H<sub>2</sub>O-stretching wavenumber values for H<sub>2</sub>O phases and for confined H<sub>2</sub>O in various microporous silicates at 298 K

Phase	Heat capacity [J/(mol·K)]	Entropy [J/(mol·K)]	H <sub>2</sub> O/OH-stretching wavenumber ( $\text{cm}^{-1}$ )	Reference for $C_p$ and $S$
steam (ideal gas)	33.59	188.84	3657 ( $v_1$ ) and 3756 ( $v_3$ )	Robie and Hemingway (1995)
liquid water	75.35	69.95	3280 ( $v_1$ ) and 3490 ( $v_3$ )	Chase (1998)
ice (hexagonal)	40.96	41.89	~3200 ( $v_{1/3}$ )	extrapolated using Giauque and Stout (1936) data
cordierite	42.2	80.5	3595 ( $v_1$ ) and 3689 ( $v_3$ )	Paukov et al. (2007)
analcime	47.9	$55.0 \pm 0.3$	~3560 to 3675	Johnson et al. (1982)
mordenite	54.4	$54.1 \pm 0.3$	~3285 to 3614	Johnson et al. (1992)
hemimorphite	$36 \pm 3$	$53 \pm 4$	~3340 to 3650	this study
heulandite	—	50.5	~3200 to 3620	Johnson et al. (1985)
paranatrolite	55.8	45.8	—	calculated from data in Paukov et al. (2007)
natrolite	—	32	~3320 and 3540	Johnson et al. (1983), from calorimetry and model calculations
scolecite	—	32	~3230 to 3590	“

deviation from ice-like behavior (see Fig. 8 in Paukov et al. 2007). Paranatrolite's  $C_p$  behavior for H<sub>2</sub>O is the most different. It shows lower  $C_p$  values than ice at  $T < 80$  K, but they increase at  $T > 80$  K such that at 298 K it has the largest  $C_p$  value listed in Table 4. Clearly, values for  $C_p$  and  $S$  of H<sub>2</sub>O in microporous silicates are variable. The macroscopic thermodynamic behavior of the various confined H<sub>2</sub>O molecules at  $0 < T < 300$  K is a function of the energies of their external (i.e., librational and translation) modes. Vibrational spectroscopic investigations have been made on most of these phases and they can be compared and analyzed in terms of their hydrogen-bonding behavior.

Consider hydrogen-bond strength described by the wavenumber of the internal stretching vibrations of the H<sub>2</sub>O molecule and its relationship to the entropy of confined H<sub>2</sub>O in the various phases in Table 4. It is known that the higher the wavenumber of the internal stretching vibrations (symmetric stretch =  $\nu_1$  and asymmetric stretch =  $\nu_3$ ), the weaker the hydrogen bonding (Jeffrey 1997). For a free H<sub>2</sub>O molecule as in steam, the internal modes lie at 3657 ( $\nu_1$ ) and 3756 cm<sup>-1</sup> ( $\nu_3$ ), while in liquid water they are about 3280 ( $\nu_1$ ) and 3490 ( $\nu_3$ ), and for ice they are around 3200 cm<sup>-1</sup> (Eisenberg and Kauzmann 1969). Thus, H bonding is strongest in ice and, of course, absent in ideal gaseous H<sub>2</sub>O. For Mg-cordierite the H<sub>2</sub>O stretching modes are at high wavenumbers, 3595 ( $\nu_1$ ) and 3689 ( $\nu_3$ ) cm<sup>-1</sup> (Paukov et al. 2007). In hemimorphite the H<sub>2</sub>O/OH stretching modes lie between 3350 and 3600 cm<sup>-1</sup> at ambient conditions (Libowitzky and Rossman 1997; Kolesov 2006). In the small-pore zeolites natrolite and scolecite stretching vibrations occur between 3200 and 3600 cm<sup>-1</sup> (Kolesov and Geiger 2006). The stretching vibrations of confined H<sub>2</sub>O in other natural zeolites are at higher wavenumbers as in analcime and mordenite (Breck 1974). Analcime, for example, shows modes between 3560 and 3675 cm<sup>-1</sup> (Velde and Besson 1981). This indicates slightly weaker H bonding than in hemimorphite and considerably weaker than in natrolite and scolecite. Thus, the strength of H bonding with its surroundings increases approximately as:

$$\text{steam} > \text{cordierite} > \text{analcime} > \text{mordenite} \geq \text{hemimorphite} \\ > \text{heulandite} > \text{natrolite} \approx \text{scolecite} > \text{liquid H}_2\text{O} > \text{ice.} \quad (3)$$

The H<sub>2</sub>O molecules in natural zeolites are also bonded to cations in their channels. Thus, quantitative comparisons with hemimorphite and the H<sub>2</sub>O phases, where H bonding is the exclusive interaction, are difficult to make. Nevertheless, the strength of the interaction between an H<sub>2</sub>O molecule and its surroundings is approximately inversely correlated to its  $S$  (Table 4). The relationship is, however, not perfect, because the external translational and librational modes largely determine  $C_p$  at low temperatures and, thus  $S$ , at 298 K. Their energies are not known, but they are affected by the H-bond interaction acting on the H<sub>2</sub>O molecules.

## ACKNOWLEDGMENTS

We thank E. Libowitzky and A. Benisek for their helpful reviews. This work was financed by the Austrian Science Fund project number P20210-N10.

## REFERENCES CITED

- Angell, C.A., Oguni, M., and Sichina, W.J. (1982) Heat capacity of water at extremes of supercooling and superheating. *Journal of Physical Chemistry*, 86, 998–1002.
- Benisek, A. and Dachs, E. (2008) The uncertainty in determining the third law entropy by the heat-pulse calorimetric technique. *Cryogenics*, 48, 527–529.
- Boero-Goates, J., Stevens, R., Hom, B.K., Woodfield, B.F., Piccione, P.M., Davis, M.E., and Navrotsky, A. (2002) Heat capacities, third-law entropies and thermodynamic functions of SiO<sub>2</sub> molecular sieves from  $T = 0$  K to 400 K. *Journal of Chemical Thermodynamics*, 34, 205–227.
- Breck, D.W. (1974) *Zeolite Molecular Sieves*, p. 771. Wiley, New York.
- Chase Jr., M.W. (1998) *NIST-JANAF Thermochemical Tables*, 4th edition, Monograph No. 9 (Part I and Part II). *Journal of Physical and Chemical Reference Data*, American Institute of Physics, Melville, New York.
- Cooper, B.J., Gibbs, G.V., and Ross, F.K. (1981) The effects of heating and dehydration on the crystal structure of hemimorphite up to 600 °C. *Zeitschrift für Kristallographie*, 156, 305–321.
- Dachs, E. and Bertoldi, C. (2005) Precision and accuracy of the heat-pulse calorimetric technique: low-temperature heat capacities of milligram-sized synthetic mineral samples. *European Journal of Mineralogy*, 17, 251–261.
- Dachs, E. and Geiger, C.A. (2006) Heat capacities and entropies of mixing of pyrope-grossular ( $\text{Mg}_3\text{Al}_2\text{Si}_5\text{O}_{12}\text{Ca}_3\text{Al}_2\text{Si}_5\text{O}_{12}$ ) garnet solid solutions: A low-temperature calorimetric and a thermodynamic investigation. *American Mineralogist*, 91, 894–906.
- Dunitz, J.D. (1994) The entropic cost of bound water in crystals and biomolecules. *Science*, 264, 670.
- Eisenberg, D. and Kauzmann, W. (1969) *The Structure and Properties of Water*. Oxford University Press, U.K.
- Giauque, W.F. and Stout, J.W. (1936) The entropy of water and the third law of thermodynamics: The heat capacity of ice from 15 to 273 °K. *Journal of American Chemical Society*, 58, 1144–1150.
- Helgeson, H.C., Delany, J.M., Nesbitt, H.W., and Bird, D.K. (1978) Summary and critique of the thermodynamic properties of rock-forming minerals. *American Journal of Science*, 278-A, 1–229.
- Hill, R.J., Gibbs, G.V., Craig, J.R., Ross, F.K., and Williams, J.M. (1977) A neutron-diffraction study of hemimorphite. *Zeitschrift für Kristallographie*, 146, 241–259.
- Jeffrey, G.A. (1997) *An Introduction to Hydrogen Bonding*, 303 p. Oxford University Press, New York.
- Johnson, G.K., Flotow, H.E., O'Hare, P.A.G., and Wise, W.S. (1982) Thermodynamic studies of zeolites: Analcime and dehydrated analcime. *American Mineralogist*, 67, 736–748.
- (1983) Thermodynamic studies of zeolites: Natrolite, mesolite and scolecite. *American Mineralogist*, 68, 1134–1145.
- (1985) Thermodynamic studies of zeolites: Heulandite. *American Mineralogist*, 70, 1065–1071.
- Johnson, G.K., Tasker, I.R., Flotow, H.E., O'Hare, P.A.G., and Wise, W.S. (1992) Thermodynamic studies of mordenite, dehydrated mordenite, and gibbsite. *American Mineralogist*, 77, 85–93.
- Kolesov, B. (2006) Raman investigation of H<sub>2</sub>O molecule and hydroxyl groups in the channels of hemimorphite. *American Mineralogist*, 91, 1355–1362.
- Kolesov, B.A. and Geiger, C.A. (2006) Behavior of H<sub>2</sub>O molecules in the channels of natrolite and scolecite: A Raman and IR spectroscopic investigation of hydrous microporous silicates. *American Mineralogist*, 91, 1039–1048.
- Libowitzky, E. and Rossman, G.R. (1997) IR spectroscopy of hemimorphite between 82 and 373 K and optical evidence for a low-temperature phase transition. *European Journal of Mineralogy*, 9, 793–802.
- Libowitzky, E., Kohler, T., Armbruster, T., and Rossman, G.R. (1997) Proton disorder in dehydrated hemimorphite: IR spectroscopy and X-ray structure refinement at low and ambient temperatures. *European Journal of Mineralogy*, 9, 803–810.
- Libowitzky, E., Schultz, A.J., and Young, D.M. (1998) The low-temperature structure and phase transition of hemimorphite,  $\text{Zn}_3\text{Si}_2\text{O}_5(\text{OH})_2\cdot\text{H}_2\text{O}$ . *Zeitschrift für Kristallographie*, 213, 659–668.
- Paukov, I.E., Moroz, N.K., Kovalevskaya, Yu.A., and Belitsky, I.A. (2002) Low-temperature thermodynamic properties of disordered zeolites of the natrolite group. *Physics and Chemistry of Minerals*, 29, 300–306.
- Paukov, I.E., Kovalevskaya, Yu.A., Rahmouni, N.-S., and Geiger, C.A. (2007) The heat capacity of hydrous cordierite at low temperatures: The thermodynamic behavior of the H<sub>2</sub>O molecule in selected hydrous micro and nanoporous silicates. *American Mineralogist*, 92, 388–396.
- Robie, R.A. and Hemingway, B.S. (1995) Thermodynamic properties of minerals and related substances at 298.15 K and 1 bar ( $10^5$  Pascals) pressure and at higher temperatures. *U.S. Geological Survey Bulletin* 2131, 461 p.
- Robinson, G.R. and Haas Jr., J.L. (1983) Heat capacity, relative enthalpy, and calorimetric entropy of silicate minerals: An empirical method of prediction. *American Mineralogist*, 68, 541–553.
- Taylor, H.F.W. (1962) The dehydration of hemimorphite. *American Mineralogist*, 47, 932–944.
- Van Hinsberg, V.J., Vriend, S.P., and Schumacher, J.C. (2005) A new method to calculate end-member thermodynamic properties of minerals from their constituent polyhedra I: enthalpy, entropy and molar volume. *Journal of Metamorphic Geology*, 23, 165–179.
- Velde, B. and Besson, J.M. (1981) Raman spectra of analcime under pressure. *Physics and Chemistry of Minerals*, 7, 96–99.

MANUSCRIPT RECEIVED NOVEMBER 6, 2008

MANUSCRIPT ACCEPTED JANUARY 5, 2009

MANUSCRIPT HANDLED BY BRYAN CHAKOUMAKOS